

Simulation and minimization of nonlinear effects in backgammon-type multi-wire gas proportional counters

A T Payne¹, J A Kimpton¹, M N Kinnane² and C T Chantler¹

¹ School of Physics, University of Melbourne, Parkville, Victoria 3010, Australia

² National Institute of Standards and Technology, Gaithersburg, MD 20899, USA

E-mail: chantler@unimelb.edu.au

Received 12 October 2008, in final form 21 November 2008

Published 30 December 2008

Online at stacks.iop.org/MST/20/025601

Abstract

The backgammon-type multi-wire gas proportional counter (MWPC) enables highly efficient detection of x-ray photons in two dimensions with good resolution and a wide range of energies and count rates. We develop a simulation which accurately describes the internal geometry of the detector and assists in the identification of several sources of nonlinear detector output. The sophistication of the model allows real solutions to be generated to minimize these effects. The result is an increase of 20% in the linear range, significant improvements to detector linearity, and improved output uniformity across both detector dimensions. These insights and methodology can be applied to other detector types and to future optimizations and developments of detector performance.

Keywords: charge attenuation, multi-wire gas proportional counter, detector modelling, x-ray spectroscopy

(Some figures in this article are in colour only in the electronic version)

1. Introduction

Since the invention of the multi-wire gas proportional counter (MWPC) by Charpak in 1968 [1], its use has been of fundamental importance not only to the field of nuclear physics, for which it was developed, but to many other areas such as x-ray spectroscopy, elementary particle physics, protein crystallography and medicine [2–5]. The ability of such devices to provide fundamental insight into so many fields of science, eventually led to the award of the 1992 Nobel Prize in physics to Charpak, ‘for his invention and development of particle detectors, in particular the multiwire proportional chamber’³. Although Charpak was fundamental to the conception of the multiwire proportional counter, motivated by the limitations of bubble and spark chambers available, he was not alone in its development.

Modelling electrostatic effects within MWPCs, especially the susceptibility to geometrical variations [6], and the

dynamics of drifting charge [7], was essential to the ongoing development of its design. Experimental investigation of the ionization processes following x-ray absorption determined the optimum operating conditions for resolution and position determination developments [8–10]. The ‘*jeu de jacquet*’ (backgammon) cathode board geometry [11], paved the way for increased spatial resolution from MWPCs via the use of capacitive charge division. Experimental developments, new data digitization and acquisition techniques [12, 13] achieved high quality results for the detection of x-rays in ‘one and a half dimensions’. Much success has also been achieved with two dimensions of sensitivity arising from the ‘modified backgammon method with weighted coupling capacitors (MBWC)’—advances not only applicable to MWPCs [14, 15], but also successful in position resolution when combined with microchannel plates (MCP) [16]. Accurate location of x-rays has also been achieved through the replacement of the cathode with microstrips [17–19], multilayer printed circuit boards [20] and polar geometry designs [21].

³ Presentation speech by Professor Carl Nordling of the Royal Swedish Academy of Sciences, translation from the Swedish text.

At the University of Melbourne, high precision tests of quantum electrodynamics (QED) have been undertaken using a Johann-type curved crystal spectrometer coupled to an electron beam ion trap (EBIT) [2, 22]. The EBIT produces highly charged uncontaminated ions, and greatly limits thermal and Doppler broadening effects, through cooling and confinement. Increased efficiency is achieved by curved crystal focussing, and the use of gravity-referenced inclinometers allows measurement of the diffraction angle to arcsecond resolution. The backgammon-type MWPC is an integral part of this system with advantages due to its large active detection area, spatial linearity and efficiency with respect to energy. By contrast, other detector types have good resolution, but the large range of x-ray energies leads to limited efficiencies, and restricted detection area. Experimental measurements of atomic transition energies using this spectrometer result in uncertainties of 20–40 ppm [2].

Nonlinear effects are inherent in most x-ray detectors, causing loss of active area, loss of resolution via broadening and reduced efficiency. The work in this paper characterizes three types of nonlinear responses. Two, namely charge attenuation and bimodal charge distribution about the mean, affect the position determination. The third, asymmetry of the electric field, influences intensity linearity. The elimination of these effects has enabled an increase of 20% in the linear range, a significant reduction of data acquisition post-processing, and improved output uniformity across both detector dimensions.

2. Detector operation

In a MWPC, the source of electrons and ions is the fill gas, which is ionized by an incoming x-ray, and separated by an applied electric field. Through optimization of parameters such as gas composition, pressure and bias voltage, a counter can be successfully operated in the proportional region whilst maximizing spatial resolution.

The detector configuration considered herein is a development on the ‘*jeu de jacquet*’ or backgammon type x-ray detector [11], and is described in detail elsewhere [23]. Whilst the detector depth was decreased from 10 mm to 7 mm in this study, the photon detection efficiency [23] was improved by 326% for $\text{CuK}\beta$ radiation—due to the use of xenon–methane gas. Two dimensions of position sensitivity are possible with the backgammon-type MWPC, one (coarse) dimension of resolution from the resistive charge distribution of electrons collected along the serpentine anode wire, the other (higher resolution dimension) from the capacitive charge distribution of positive ions collected on the two plates of the backgammon board (figure 1). It is this higher resolution dimension which is aligned with the plane of dispersion when the detector is operated as part of the curved crystal spectrometer.

The electronics and data acquisition system (DAQ) employed in the operation of the backgammon-type MWPC are described in full elsewhere [24]. In essence, the four output signals of the MWPC, two anode and two cathode, are integrated by independent charge sensitive pre-amplifiers, then

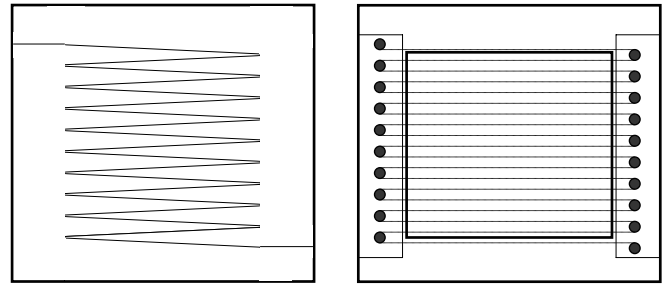


Figure 1. Shows the backgammon cathode board (left) as divided into two capacitor plates with $100\ \mu\text{m}$ channel separation. The anode wire configuration (right) is shown as configured for previous work with the detector [23].

amplified and balanced by independent shaping amplifiers. Only signals deemed to be in coincidence are representative of real x-ray photoionization events, and as such are digitized and recorded along with timing information.

3. Detector modelling

An accurate geometrical representation of the MWPC elements was constructed for each intended experiment. These representations were used as the basis for all simulations. The model accurately reproduces the four output signals (i.e. the two anode signals A and B and two cathode signals C and D) of the actual detector for an x-ray incident at any Cartesian coordinate (x, y) within the proportional chamber, hence mapping,

$$(x, y) \longrightarrow (x'(C, D), y'(A, B)).$$

Along the anode sensitive dimension, an event within the active region of the detector drifts towards an anode segment, locating the centroid of avalanche formation. As the resistance of the wire is proportional to length, the distance to each end of the anode wire is calculated, and the reciprocals used as the signals A and B to determine the resistive charge division. The output position is then,

$$y' = \frac{A}{A + B}.$$

In the cathode dimension, the model works by generating a mesh of triangles to represent the geometry of the backgammon board, described as the vertices of polygons. An incident x-ray event is represented by a rectangular distribution of ions surrounding the location of avalanche formation. The radius of this distribution reflects changes in the footprint size. A projection of each charge distribution is made onto the mesh of triangles, and the projected area calculated—proportional to the charge deposited on each side of the backgammon board (defining signals C and D). The position along the cathode axis x' , is determined by capacitive charge division:

$$x' = \frac{C}{C + D}.$$

This detector model accurately replicates nonlinear effects as observed experimentally in previous MWPC detector designs [13, 15]. Figure 2 is an example MWPC output for a $\text{CuK}\beta$ characteristic transition prior to this work. Ideally

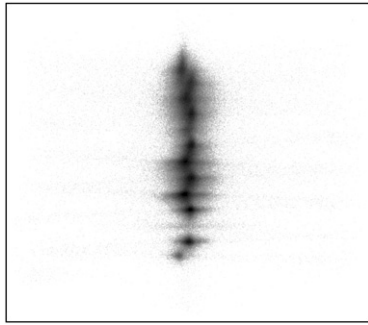


Figure 2. Example $\text{CuK}\beta$ linearity test data from a previous design. Nonlinear effects such as curvature at the top and bottom, and wire-by-wire displacement about the mean vertical position are visible.

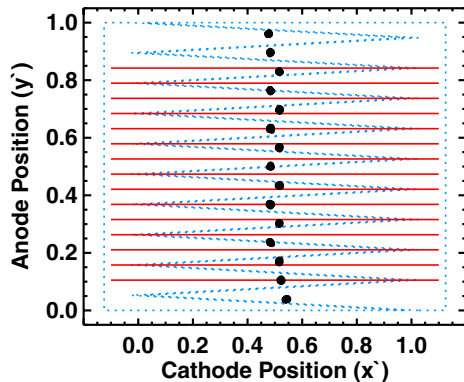


Figure 3. Shows an example backgammon-type MWPC model output for a detector of 16 anode segments. Two nonlinear effects are visible in the output, manifest as curvature at the top and bottom and bimodal displacement from the mean vertical position.

the detector image should represent the shape of the incident spectral line which was a straight, vertical line in this instance. Clearly observable is the effect of curvature of the straight incident spectral line towards the top and bottom of the line, where the outputs of the last anode segments are displaced along the horizontal (energy) axis. Also visible is the displacement about the mean vertical position on a wire-by-wire basis. Each of these observed effects lead to output broadening and difficulties in data processing.

An example detector model is shown in figure 3, generated for 1000 photons distributed upon a single vertical line in the centre of the detector. The backgammon cathode board is shown as dashed lines, the placement of 16 anode wire segments by solid lines, and the location of the output ‘counts’ shown in black dots. Two nonlinear effects are readily visible in this output, the curvature of the vertical line at the top and bottom as well as the bimodal displacement from the mean vertical position. The model has allowed determination of the cause of such effects and characterization of their form and magnitude, and has also enabled their minimization through detailed simulation of model parameters.

4. Configuration modelling and experiment

4.1. Charge attenuation

The modelling of various anode wire configurations and different ion cloud distributions allowed accurate

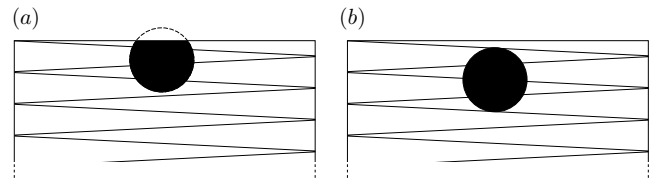


Figure 4. Diagram illustrating the cause of charge attenuation. (a) The avalanche of charge is partially insulated from the capacitor by the MACOR frame—resulting in charge attenuation. (b) The ion cloud remains clear of the MACOR frame allowing correct position determination.

determination of the cause of curvature at the top and bottom of the MWPC.

This curvature is observed in configurations where the ions interacted with the MACOR anode wire mounting frame. This effect is caused by the avalanche of charges not being deposited uniformly on to the backgammon cathode, due to the perimeter of the MACOR frame insulating the capacitor from the ion drift (figure 4(a)). Hence, the ability of the capacitive charge distribution method to accurately locate the centroid of avalanche formation is exceeded, and curvature of the straight line distribution of x-rays results. No such problem occurred for models in which there existed a sufficient standoff region between the active anode segments and the insulated boundary for a particular footprint size (figure 4(b)).

The experimental set-up used for each configuration study utilized a MacScience rotating anode x-ray source, operated with a copper target at 20 keV and 10 mA. The full copper spectrum was simply attenuated by series of lead and aluminium foils followed by a 1 mm wide vertical slit attached directly to the face of the detector.

A detector was constructed in which the last wired anode segments were completely clear (10 mm) of the MACOR frame. This configuration was expected to exhibit some nonlinear response along the anode sensitive axis as the last wires will not experience the same electric field as the central wires. Figure 5 shows the elimination of curvature due to charge attenuation by this design, however the effect of irregular field distribution at the last two segments is observed—characterized by a disproportionate number of counts collected by the last two segments at the top and bottom of the detector.

4.2. Field asymmetry

A uniform electric field environment around each anode wire is essential for linear intensity response across the face of the detector. Whilst this is inherent in an infinite array of equally spaced wires in a perfectly symmetric chamber, it is not physically realizable. The last segments of the anode wire must experience a different electric field to a segment located centrally. Large diameter low resistance wires were used to replace the last active wire segments to guard against field asymmetry. This helps avoid charge attenuation at the upper and lower boundaries of the detector as these wires are unlikely to form sufficiently large avalanches due to their size and reduced electric field density [6]. Therefore

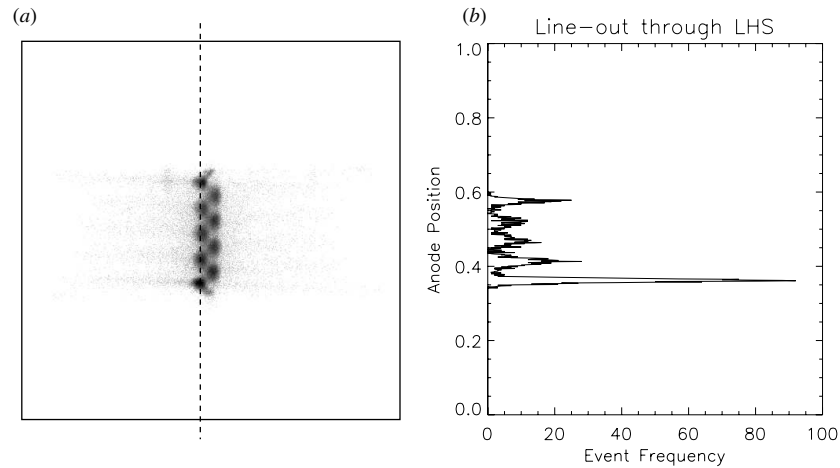


Figure 5. Example experimental output showing curvature effect eliminated, however the effect of field asymmetry is now apparent in the disproportionate number of counts collected at the top and bottom anode segments—characterized in the grey-scale image (a) by more intense (darker) output. (b) The line-out through the dashed line shown further demonstrates this.

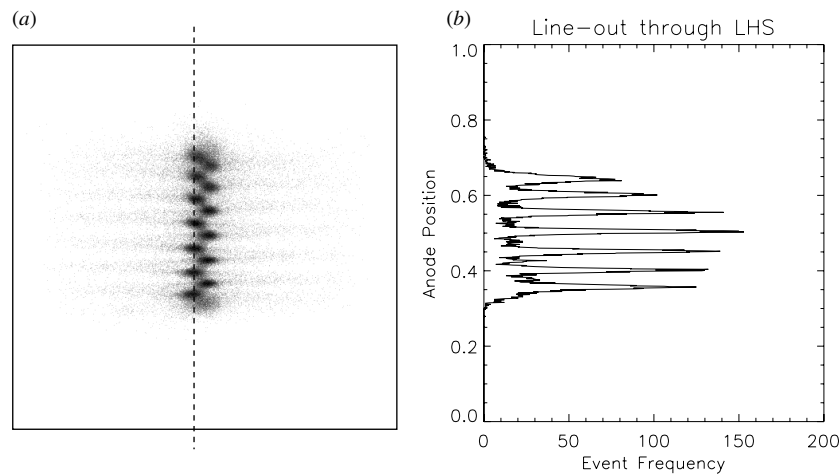


Figure 6. (a) Example of experimental output showing the elimination of both curvature and field asymmetry effects. (b) The line-out through the dashed line shown demonstrates the success of the new geometry.

the large diameter ‘guard-wires’ maintain field uniformity, without adding appreciably to the total resistance of the anode configuration [25].

The detector design was modified in a further experiment with the addition of guard wires at each end of the anode assembly. It is clear from the uniformity in the wire signal intensity shown in figure 6 that the effect of irregular field distribution at the end segments is thereby overcome.

4.3. Bimodal distribution about the mean position

For each design shown previously, the response from adjacent wire segments consistently exhibits a bimodal shift on a wire-by-wire basis about the mean vertical line position. This effect leads to a shift in apparent centroid location, such that ‘odd’ numbered segments result in a shift to the left, while ‘even’ segments shift to the right. As such, for spectra collected by the backgammon MWPC, this bimodal distribution of events is often linearized as an initial step of data analysis, which introduces a significant computational overhead. The

spectrum to be straightened is (for example) fitted row-by-row, a mean centroid calculated and the deviation of the centroid of each row from the mean used as the correction. The correction of systematic image deformations and the distinction between anode segments leads to important improvements in the analysis of backgammon-type MWPC data [13, 26].

The cause of the bimodal distribution was uncovered by modelling the detector design for the optimization of anode configuration. The underlying phenomenon responsible was found to be the positioning of the anode wires with respect to the interleaved sawtooth pattern of the cathode board. In the previous anode sub-frame design, each wire segment was lined-up with the point of a backgammon tip. As the backgammon pattern was of a 4 mm pitch and the wire spacing set at 2 mm, alternating wire segments were aligned with alternating plates of the cathode capacitor. Thus an avalanche necessarily forming around a single wire segment would lead to a preferential deposit of positive ions to one side of the capacitor.

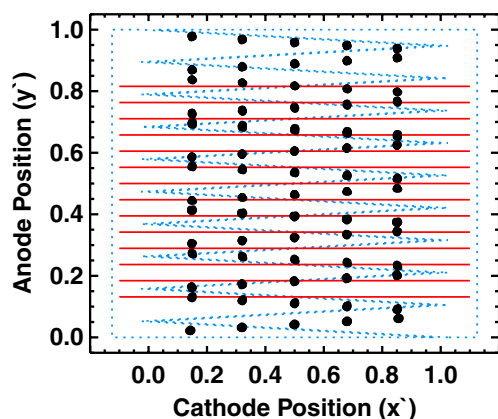


Figure 7. The model output for five straight line x-ray distributions incident vertically upon the detector. Note that only the last (bottom) wire is displaced from the line by the effect of charge attenuation.

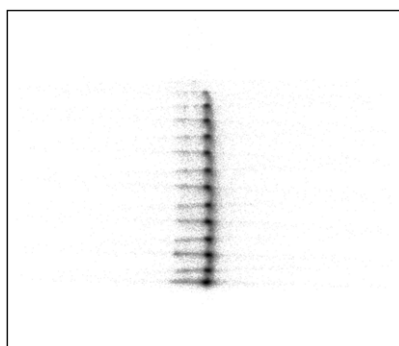


Figure 8. Sample output of $\text{CuK}\beta$ spectral line incident on the centre of the detector, showing the removal of the bimodal distribution about the mean position. Note the shift in the last wire as predicted by the model.

Several detector configurations were modelled where the anode wires crossed the cathode capacitor plates at different locations. The optimum configuration where the bimodal distribution was minimized was when the anode segments crossed the exact midpoint of the backgammon ‘teeth’. The result of this is that both capacitor plates receive the proportionate charge for any reasonable avalanche size.

Figure 7 illustrates a sample model output of this new design, showing a series of five straight line distributions of photons incident vertically upon the detector. From the location of the reconstructed model events it is clear that the bimodal distribution has been minimized and now appears negligible (cf model bimodality in figure 3). Also visible in the model output is the effect of changes in spacing between adjacent anode segments at the left and right extremes of the detector. This is an effect of the anode charge division method equating a displacement along the length of a wire segment with a displacement along the anode sensitive axis.

The detector output for a $\text{CuK}\beta$ spectral line (figure 8) shows the successful removal of the bimodal distribution, using the new anode configuration. An improvement in the raw projected resolution by a factor of 1.86 is a significant result for the detector. The effect of charge attenuation has re-appeared in this design, manifest as a slight curvature in the

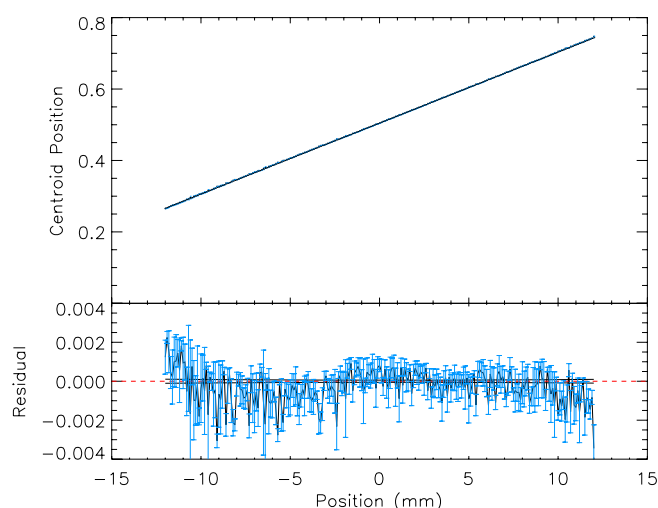


Figure 9. Fractional centroid position across the detector. Error bars are the standard percentage errors in the determined centroid position. The solid lines are the standard error envelope of the determined linear fit.

last (bottom) anode segment. Close inspection of the model for this configuration (figure 7), reveals that this effect was due to the clearance between the extreme wires and the MACOR frame boundary (5.6 mm at the top of the frame and 5.4 mm at the bottom). This is further evidence of the accuracy of the computer simulation in predicting actual detector operation.

5. Linearity

An important attribute of the backgammon-type MWPC is its spatial linearity over a large area. Prior to testing the spatial linearity, a set of optimized operating conditions (gas composition, pressure and anode bias voltage) were determined. The MWPC was filled with xenon–methane (10% methane in xenon) at 1.91 atm and operated with an anode bias voltage of 2400 volts. To test the spatial linearity of the new anode configuration a MacScience rotating anode x-ray source was employed to produce a copper spectrum, monochromated to $\text{CuK}\beta$ by a $\text{Si}(1\ 1\ 1)$ channel-cut crystal. Four hundred $\text{CuK}\beta$ characteristic spectra were collected in 100 μm steps along the axis of cathode sensitivity across the 40 mm window of the detector.

Each $\text{CuK}\beta$ spectrum was fitted using the sum of two Lorentzian profiles by a Levenberg–Marquardt least-squares algorithm, the centroid determined and compared with the detector position on the linear stage. Figure 9 illustrates the resulting spatial linearity with residual from a linear fit. Standard errors in the determination of centroid position are shown as error bars, while the standard error envelope of the linear fit is shown in solid lines.

This detector configuration indeed provides a large region of linear operation, with a 20% extension of the linear active region to 24 mm as compared to previously constructed detectors, achieved through the elimination of the bimodal distribution and other sources of nonlinear response. Across

this central 24 mm the detected location as a function of the illuminated position is

$$x' = (0.019873 \pm 4 \times 10^{-6})x(\text{mm}) + (0.50508 \pm 3 \times 10^{-5}).$$

The maximum of the standard percentage errors on the determined linear fit (envelope shown) is only 0.010% or 2.4 μm . This measure indicates that, subject to noise and statistics, a broad feature or wide separation of peaks can be resolved to very high accuracy.

A regional differential nonlinearity of 0.068% was defined as the average deviation of the detected centroid positions from the linear fit. This is the most useful measure of spatial linearity, looking at the pointwise excursions over the operational area and estimating the typical error of a single channel position determination.

The maximum fractional excursion is usually due to a few outliers from measurement error rather than from the full range linearity, but is a good estimate of the worst possible performance. Calculated as the maximum deviation of a detected position from the linear fit a value of 0.345% was found. This is comparable with the previous best result [23] despite limited statistics and without data pre-processing within the operational area.

The fractional uncertainty on the fitted gradient of 0.019% and offset uncertainty of 0.005% represent significant improvements compared with earlier designs [11–13].

The improved design developed herein has successfully minimized the strong wire-by-wire bimodal distribution. A significant additional outcome of removing this source of nonlinear response is the reduction of data processing overheads and the involved software linearization often required. Further detailed characterization of the detector is continuing. This work yields an improved understanding of the charge cloud footprint mechanism, its effect on the spatial linearity of the detector, and the potential for further linearity enhancement.

6. Conclusion

The model developed has enabled detailed experimental simulation, clearly illuminating the cause of several nonlinear effects observed in the backgammon-type MWPC operation. Insight gained through simulation provides justification for new experimental designs to successfully minimize or eliminate such effects, and also serves to help characterize detector response.

Two prevalent nonlinear effects leading to broadening of the backgammon MWPC output were effectively eliminated through a systematic anode reconfiguration. Spectral line curvature due to charge attenuation by the MACOR frame was resolved by the estimation of apparent footprint size and the reduction of end-affected anode segments. The effect of electric field asymmetry at the end wires was also optimized by the addition of guard wires to the design.

An improved anode configuration led to the removal of a source of broadening and significant computational overhead from the bimodal distribution of events about the true position of the spectral line. Preliminary results for this improved

design are excellent with an increased detector range of 20%, increased photon detection efficiency by 326%, and spatial linearity in-line with or improving on prior detector designs. Most important is that channel-summed measures are now representative of the uniformity along the columns or across each row of the detector. This represents both a significant detector development, simplification of assessing linearity in raw and processed data, and a methodology for optimizing future detector developments of this and related types.

Acknowledgments

We wish to thank Mr L F Smale for his development of the model and assistance. We would also like to thank the Australian Research Council for their funding of the project.

References

- [1] Charpak G, Bouclier R, Bressani T, Favier J and Zupancic C 1968 The use of multiwire proportional counters to select and localize charged particles *Nucl. Instrum. Methods* **62** 262–8
- [2] Chantler C T, Paterson D, Hudson L T, Serpa F G, Gillaspay J D and Takács E 2000 Absolute measurement of the resonance lines in heliumlike vanadium on an electron-beam ion trap *Phys. Rev. A* **62** 042501
- [3] Assamagan K *et al* 1999 Time-zero fission-fragment detector based on low-pressure multiwire proportional chambers *Nucl. Instrum. Methods Phys. Res. A* **426** 405–19
- [4] Fuzi J 2008 Spectral accuracy of multiwire proportional counter neutron detectors in time-of-flight regime *Meas. Sci. Technol.* **19** 034028
- [5] Irving M, Lombardi V, Piazzesi G and Ferenczi M A 1992 Myosin head movements are synchronous with the elementary force-generating process in muscle *Nature* **357** 156–8
- [6] Erskine G A 1972 Electrostatic problems in multiwire proportional chambers *Nucl. Instrum. Methods* **105** 565–72
- [7] Erskine G A 1982 Charges and currents induced by moving ions in multiwire chambers *Nucl. Instrum. Methods* **198** 325–36
- [8] Smith G C, Fischer J and Radeka V 1984 Photoelectron range limitations to the spatial resolution for x-rays in gas proportional chambers *IEEE Trans. Nucl. Sci.* **NS-31** 111–5
- [9] Fischer J, Radeka V and Smith G C 1986 X-ray position detection in the region of 6 μm RMS with wire proportional chambers *Nucl. Instrum. Methods Phys. Res. A* **252** 239–45
- [10] Fischer J, Radeka V and Smith G C 1986 Position detection of 17–25 keV x-rays in krypton and xenon with a resolution of 18–50 μm (FWHM) *IEEE Trans. Nucl. Sci.* **33** 257–60
- [11] Allemand R and Thomas G 1976 Nouveau détecteur de localisation *Nucl. Instrum. Methods* **137** 141–9
- [12] Duval B P, Barth J, Deslattes R D, Henins A and Luther G G 1984 Position-sensitive x-ray detector *Nucl. Instrum. Methods Phys. Res.* **222** 274–8
- [13] Luther G G, Cowan P L, Henins A and Brennan S 1986 New two dimensional position sensitive proportional detectors using charge division *Nucl. Instrum. Methods Phys. Res. A* **246** 537–40
- [14] Mizogawa T, Awaya Y, Isozumi Y, Katano R, Ito S and Maeda N 1992 New readout technique for two-dimensional position-sensitive detectors *Nucl. Instrum. Methods Phys. Res. A* **312** 547–52
- [15] Mizogawa T, Sato M and Awaya Y 1995 Application of the 'MBWC' two-dimensional position readout technique to a

- multiwire proportional counter *Nucl. Instrum. Methods Phys. Res. A* **366** 129–36
- [16] Mizogawa T, Sato M, Yoshino M, Itoh Y and Awaya Y 1997 A two-dimensional position-sensitive anode for microchannel plates based on the ‘MBWC’ technique *Nucl. Instrum. Methods Phys. Res. A* **387** 395–400
- [17] Gatti E, Longoni A, Okuno H and Semenza P 1979 Optimum geometry for strip cathodes or grids in MWPC for avalanche localization along the anode wires *Nucl. Instrum. Methods* **163** 83–92
- [18] Radeka V and Boie R A 1980 Centroid finding method for position-sensitive detectors *Nucl. Instrum. Methods* **178** 543–54
- [19] Piuz F, Roosen R and Timmermans J 1982 Evaluation of systematic errors in the avalanche localization along the wire with cathode strips read-out MWPC *Nucl. Instrum. Methods* **196** 451–62
- [20] Barbosa A F 1996 Use of a multilayer printed circuit board as the position sensing electrode in an MWPC *Nucl. Instrum. Methods Phys. Res. A* **371** 368–74
- [21] Martin C, Jelinsky P, Lampton M, Malina R F and Anger H O 1981 Wedge-and-strip anodes for centroid-finding position-sensitive photon and particle detectors *Rev. Sci. Instrum.* **52** 1067–74
- [22] Chantler C T, Kinnane M N, C-H Su and Kimpton J A 2005 Characterisation of $K\alpha$ spectral profiles for vanadium, component redetermination for scandium, titanium, chromium and manganese, and development of satellite structure for $Z = 21$ to $Z = 25$ *Phys. Rev. A* **73** 012508
- [23] Kimpton J A, Kinnane M N and Chantler C T 2006 Development of backgammon-type multiwire proportional counters for the detection of x rays *Rev. Sci. Instrum.* **77** 083102
- [24] Kimpton J A *et al* 2007 Data acquisition system development for the detection of x-ray photons in multi-wire gas proportional counters *Nucl. Instrum. Methods Phys. Res. A* **580** 246–9
- [25] Wilkinson D H 1950 *Ionization Chambers and Counters* (Cambridge: Cambridge University Press)
- [26] Kinnane M N, Kimpton J A, Jonge M D de, Makonyi K and Chantler C T 2005 The correction of systematic image deformations inherent to two-dimensional proportional counters *Meas. Sci. Technol.* **16** 2280–6